Chapter 1

Contact Mechanics of Rough Surfaces in Hermetic Sealing Studies

Peter Ogar, Sergey Belokobylsky and Denis Gorokhov

Additional information is available at the end of the chapter

http://dx.doi.org/10.5772/intechopen.72196

Abstract

It is indicated that the sealing capacity depends on the contact characteristics—the relative contact area and the gap density in the joint. To determine the contact characteristics, a discrete roughness model is used in the form of a set of spherical segments, the distribution of which in height is related to the bearing curve described by the regularized beta function. The contact of a single asperity is considered with taking into account the influence of the remaining contacting asperities. The equations for determining the relative contact area and gap density in the joint depending on the dimensionless force parameters for elastic and elastic-plastic contacts are provided.

Keywords: contact mechanics, hermetic sealing studies, rough surface, spherical asperity, discrete model, elastic contact, elastic-plastic contact, hardening power law, relative contact area, gaps density, sealing joint, tightness

1. Introduction

Tightness is the property of the joints to provide an acceptable leakage value, determined from the conditions of normal operation of various systems and equipment, human safety, and environmental protection. To quantify the tightness, the leakage rate is used, that is, the mass or volume of the medium per unit time per unit length along the SJ's perimeter. By 'sealing joint' (SJ), we mean a set of details that form a structure to ensure tightness.

The SJ's tightness is provided by loading with a compressive load (the contact sealing pressures), which is largely determined by the stress-strain state in the contact area and depends on the contact interaction of the rough surfaces. The main contact characteristics ensuring SJ's tightness are the approaching of rough surfaces, the relative contact area, the density of gaps in the joint, and the degree of fusion of contact spots of single asperities. Depending on the

materials' properties and microgeometry parameters, there are elastic, viscoelastic, elastic-plastic, and rigid-plastic contacts.

At present, to solve the tribology problems, we need to use the roughness models and the rough surfaces contacting theory developed by the authors [1, 2] and their followers. However, the use of such models to solve the problems in hermetic sealing studies leads to significant errors, which is explained by the following:

1. the contact pressures of the sealing are approximately 1–2 orders of magnitude higher than for friction and at that, it is necessary to be taken into account the mutual influence of the contacting asperities;
2. in the sealing joint, all the asperities's contacting is possible, which requires the description of the whole bearing profile curve but not only its initial part, as in [2];
3. when determining the gaps volume (or density), the displacements of the points of the asperities surfaces have not been taken into account; and
4. the extrusion of the material into the intercontact space under elastic-plastic contact has not been taken into account.

Therefore, to describe the SJ, a rough surface model is required that adequately describes the real surface and corresponds to the whole bearing curve, and not just its initial part. In addition, in order to improve the accuracy of the calculation of the contact characteristics, the discrete model of a rough surface must be taken into account, the real distribution of dimensions of microasperities and the mutual influence. The criterion of plasticity must take into account the general stress-strain state when contacting of a rough surface and not just of a single asperity. In most cases, the contact of metallic rough surfaces is elastic-plastic, therefore, to determine the contact characteristics, it is necessary to take into account the parameters of material hardening.

To estimate the SJ's sealing property, in [3, 4], the nondimensional permeability functional is used

$$C_u = \frac{\Lambda^3 \upsilon_k}{4(1-\eta)^2}, \tag{1}$$

where Λ is the gaps density in the joint; η is the relative contact area; υ_k is the probability of a medium flowing, which depends on the single contact spots fusion.

All the parameters that appear in Eq. (1) depend on the parameters of microgeometry and dimensionless force parameters f_q or $\overline{q}_\sigma$, the determination of which is given in the following sections.

The purpose of the given research is to develop methods for calculating the contact characteristics that ensure the given tightness of the immobile joints with taking into account the complex of functional parameters of the sealing surfaces and mutual influence of asperities.

http://dx.doi.org/10.5772/intechopen.72196

2. Discrete model of the rough surface

We consider that the initial data for the model representation of a rough surface are parameters of roughness according to ISO 4287–1997, ISO 4287/1–1997: maximum roughness depth $R_{\max}$, arithmetic mean deviation of the profile R_a, root-mean-square deviation of the profile R_q, mean height of the profile elements R_p, mean width of the profile elements S_m, bearing profile curve t_p, and bearing profile curve on the midline t_m. Thus, the standard parameters of the roughness for the developed model must coincide with the corresponding parameters of the real surface.

To describe the entire rough surface, it is required to know one of two functions:

$$\eta_u(\varepsilon) = \frac{A_u}{A_c} \text{ or } \varphi_n(u) = \frac{n_u}{n_c}, \tag{2}$$

where A_u is the material cross-sectional area at a relative level $\varepsilon = h/R_{\max}$; A_c is the contour area; n_u is the number of asperities whose peaks are located above the level u; $n_c = A_c/A_{ci}$ is the total number of asperities; and A_{ci} is the area due to a single asperity.

According to ISO 4287–1997, parameters of roughness are determined from profilograms and the functions describing the distribution for the profile t_p and the surface $\eta_u(\varepsilon)$, but it is not fulfilled for the peaks and valleys asperities distribution functions of the profile $\varphi_{nl}(u_l)$ and the surface $\varphi_n(u)$, then the model is based on the bearing profile curve.

Let us assume that the function $\eta_u(\varepsilon)$ is monotonic and twice differentiable. A rough surface (**Figure 1**) is a set of asperities in the form of spherical segments of radius r and height $\omega R_{\max}$, and base radius $a_c = \sqrt{A_{ci}/\pi}$. It is necessary to find such a function $\varphi_n(u)$ for which the distribution of the material in the rough layer corresponds to the bearing surface curve.

The cross-section of the i-th asperity at the level ε is

$$A_{ri} = 2\pi r R_{\max}(\varepsilon - u), \tag{3}$$

where u is the relative distance from the peaks level to the peak of the i-th asperity.

The number of peaks in the layer du and at a distance u is equal to

$$dn_r = n_c \varphi_n'(u) du. \tag{4}$$

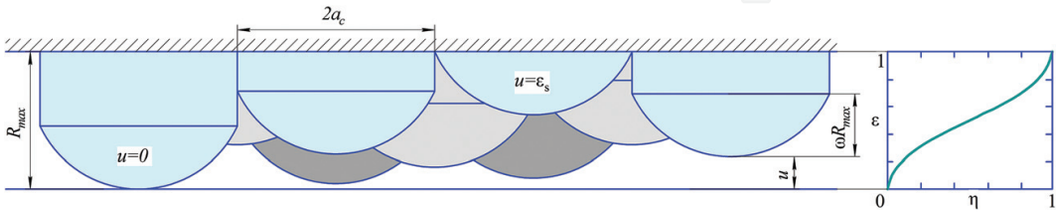

Figure 1. The scheme and the bearing curve of a rough surface.

Then, $A_u = A_r = 2\pi r R_{\max} n_c \int_0^{\varepsilon} \varphi_n'(u)(\varepsilon - u)du$;

$$\eta_u(\varepsilon) = \frac{A_r(\varepsilon)}{A_c} = C\int_0^{\varepsilon}(\varepsilon - u)\varphi_n'(u)du,\ C = \frac{2\pi r R_{\max} n_c}{A_c}. \tag{5}$$

Further, we have

$$\eta(\varepsilon) = C\left(\varepsilon\int_0^{\varepsilon}\varphi_n'(u)du - \int_0^{\varepsilon}u\varphi_n'(u)du\right) = C\left(\varepsilon\varphi_n(\varepsilon) - u\varphi_n(u)\Big|_0^{\varepsilon} + \int_0^{\varepsilon}\varphi_n(u)du\right),$$

$$\eta(\varepsilon) = C\int_0^{\varepsilon}\varphi_n(u)du. \tag{6}$$

Twice differentiating the left and right sides of ε, we have

$$\eta'(\varepsilon) = C\varphi_n(\varepsilon), \quad \eta''(\varepsilon) = C\varphi_n'(\varepsilon); \tag{7}$$

$$\varphi_n(\varepsilon) = \frac{\eta'(\varepsilon)}{C}, \quad \varphi_n'(\varepsilon) = \frac{\eta''(\varepsilon)}{C}. \tag{8}$$

To describe the bearing surface curve, we use the regularized beta function:

$$t_p(\varepsilon) = \eta(\varepsilon) = I_\varepsilon(p,q) = \frac{\mathrm{B}_\varepsilon(p,q)}{\mathrm{B}(p,q)}, \tag{9}$$

where

$$p = \left(\frac{R_p}{R_q}\right)^2\left(\frac{R_{\max} - R_p}{R_{\max}}\right) - \frac{R_p}{R_{\max}},\ q = p\left(\frac{R_{\max}}{R_p} - 1\right). \tag{10}$$

$\mathrm{B}_\varepsilon(\alpha,\beta)$ и $\mathrm{B}(\alpha,\beta)$ are the incomplete and complete beta-functions.

Double differentiating Eq. (9), from Eq. (8), for the function and the distribution density of the asperities, we have

$$\varphi_n(u) = \frac{\eta_u'(u)}{C} = \frac{u^{p-1}(1-u)^{q-1}}{\varepsilon_s{}^{p-1}(1-\varepsilon_s)^{q-1}}; \tag{11}$$

$$\varphi_n'(u) = \frac{\eta''{}_u(u)}{C} = \frac{u^{p-2}(1-u)^{q-2}[(p-1)(1-u) - (q-1)u]}{\varepsilon_s^{p-1}(1-\varepsilon_s)^{q-1}}. \tag{12}$$

The relative height of the spherical asperity is $\omega = 1 - \varepsilon_s$ and the radius of spherical asperity is $r = a_c^2/(2\omega R_{\max})$.

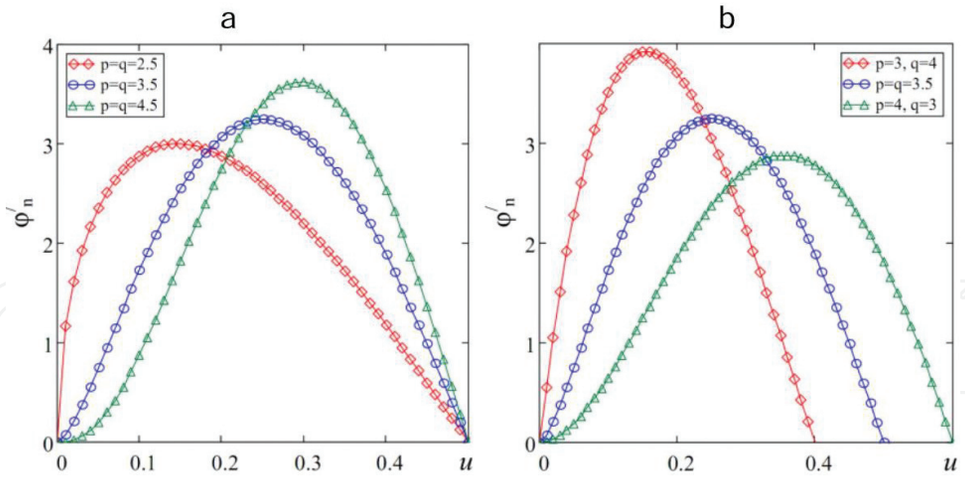

Figure 2. The distribution densities of asperities for different values of p and q.

This section describes a model of a rough surface in the form of a set of spherical asperities with constant radii and heights. More complex models with asperities with variable radii and heights are given in work [3, 4].

The contact of two rough surfaces $z_i(x, y)$ can be represented as a contact of an equivalent rough surface $z(x, y) = \sum_{i=1}^{2} z_i(x, y)$ and a flat surface. The parameters of the microgeometry of an equivalent surface are given in [3, 4].

3. Description of contact of a single asperity

3.1. Contact of a spherical asperity and the low-modulus half-space

Elastic contact occurs when low-modulus materials are used, which are used widely in sealing technology in the form of coatings or individual details [3, 5]. According to the strength criteria, the construction materials belong to the low-modulus materials if the values of the elastic moduli $E < 10^3$ MPa [6]. When contacting metallic rough surfaces, elastic contact is possible for high surface cleanliness classes and large values of the yield strength of the material.

As shown by experiments [7, p. 179] with polymeric interlayers (a coating on one of the conjugate details), loaded by [1] compressive stresses, the real touching area tends to be a constant value, depending on the physico-mechanical properties of the interlayer material.

During elastic contact, the mutual influence of discretely loaded sections leads to the growth retardation of the contact area [3]. It is reflected in the Bartenev-Lavrentyev's formula [7]

$$\eta = 1 - \exp\left(-b\frac{q}{E}\right), \tag{13}$$

where b is the coefficient depending on the surface quality, q_c is the contour contact pressure, and E is the elastic modulus. As it follows from Eq. (13), $\eta \to 1$ for $q \to \infty$.

The question of the influence of neighboring asperities in the case of elastic contact was considered in [8, 9], where the mutual influence is replaced by the action of equal concentrated forces located at the nodes of the hexagonal lattice.

According to the Saint-Venant's principle, at a point sufficiently distant from the region of application of the load, the stresses and deformations do not depend on the nature of the load distribution in its application area, in [10, 11]. Using the principle, the influence of the other contacting asperities is replaced by the action of a uniformly distributed load in some circular area. It allows considering the problem posed as an axisymmetric problem.

Let us consider the contact of a single absolutely rigid spherical asperity of radius r, whose peak is located at a distance $uR_{\max}$ from the peaks line of a rough surface with an elastic half-space in the system of cylindrical coordinates z, ρ, and φ with origin at the point O (**Figure 3**).

From an analysis of the numerous solutions of contact problems in the theory of elasticity and plasticity, it follows that a change of the distribution of external loads near the contact area

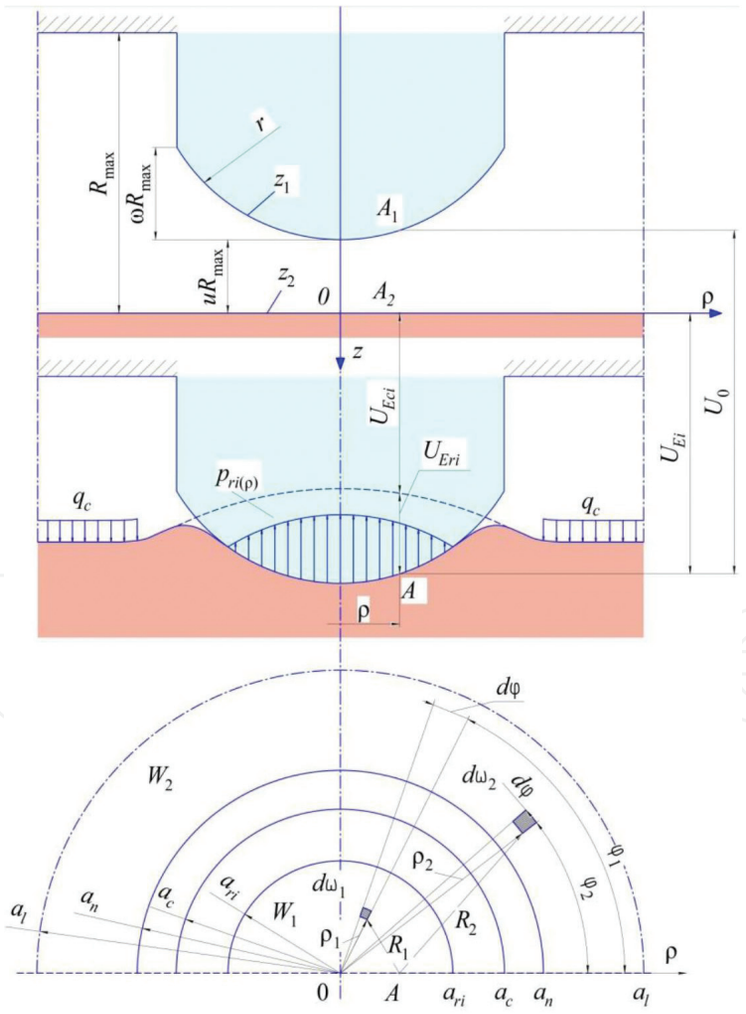

Figure 3. Scheme of contact of a single asperity.

under constancy of its average intensity leads to insignificant changes only near the boundary of the contact area.

Then, taking into account, the nature of the mutual location of the individual contact spots, the influence on the contact characteristics of an individual asperity within the circular contact area $W_1(\rho = \overline{0, a_{ri}})$ and the circular unloaded area $W(\rho = \overline{a_{ri}, a_n})$ on the remaining contact spots will be equivalent to the effect of the uniformly distributed load q_{cn} acting in the circular area $W_2(\rho = \overline{a_n, a_l})$, and the assigned problem may be regarded as an axisymmetric (**Figure 3**). The size of the unloaded area a_n depends on the number of contacting asperities and with increasing applied load, it decreases from a_l to a_c.

The solution of this problem is given in Ref. [11]. Studies on the effect of the parameter $k_a = a_n/a_c$ on the relative contact area show only 4% increase of last one; therefore, with a margin to tightness ensure, we will give a solution for $k_a = 1$ or $a_n = a_c$ below.

Let A_1 and A_2 be two points on the surface of the circular contact area W_1. The A_1 and A_2 coming into contact after application of the compressive load. Since the total normal displacement U_0 of the point A_1 is constant for any point in area W_1, we have

$$U_0 = U_E + z_1 = U_{Eri} + U_{Eci} + z_1, \tag{14}$$

where U_{Eri} is the normal contact displacement under the pressure p_{ri} acting in the region W_1; U_{Eci} is the normal displacement under the pressure q_{cn}; and z_1 is the equation of the surface of a spherical asperity in an unloaded state.

As for the real surfaces, $r >> R_{\max}$, then

$$z_1 = -uR_{\max} - \frac{\rho^2}{2r}. \tag{15}$$

Elementary displacements dU_{Eri} and dU_{Eci} under pressures q_{ri} and q_c acting on elementary areas dw_1 and dw_2, respectively, are determined by [12]:

$$dU_{Eri} = \frac{\theta q_{ri}(\rho_1)}{\pi R_1} dw_1,\ dU_{Eci} = \frac{\theta q_{cn}}{\pi R_2} dw_2; \tag{16}$$

where $R_j^2 = \rho^2 + \rho_j^2 - 2\rho\rho_j \cos\varphi_j$, $j = 1, 2$; $\rho \equiv \rho_i$; $\theta = (1 - \nu^2)/E$, ν is Poisson's ratio; $dw_1 = \rho_1 d\rho d\varphi$; and $dw_2 = \rho_2 d\rho d\varphi$.

After integrating Eq. (16), we have

$$U_{Eri} = \frac{\theta}{\pi} \int_{W_1} \frac{p_{ri}(\rho) dw_1}{R_1}, \tag{17}$$

$$U_{Eci} = \frac{4}{\pi} \theta q_c \left[a_l \mathrm{E}\left(\frac{\rho_i}{a_l}\right) - a_c \mathrm{E}\left(\frac{\rho_i}{a_c}\right) \right], \tag{18}$$

where $E(x)$ is the complete elliptic integral of the second kind.

From Eq. (15), taking into account Eqs. (16)–(18), we have

$$\int_{W_1} \frac{p_{ri}(\rho)dw_1}{R_1} = f(\rho_i), \tag{19}$$

$$f(\rho_i) = \frac{\pi}{\theta}\left(U_0 - uR_{\max} - \frac{\omega R_{\max}\rho_i^2}{a_c^2}\right) - 2\pi q_c\left[a_l - \frac{2}{\pi}E\left(\frac{\rho_i}{a_c}\right)\right]. \tag{20}$$

The Eq. (19) is the basic equation of an axisymmetric contact problem. The common decision of Eq. (19) is [13].

$$p_{ri}(\rho_i) = -\frac{1}{2\pi}\int_{\rho_i}^{a_{ri}} \frac{F(s)ds}{\sqrt{s^2-\rho_i^2}},\ P_i = -\frac{2}{\pi}\int_0^{a_{ri}} \frac{f'(\sigma)\sigma^2 d\sigma}{\sqrt{a_r^2-\sigma^2}}, F(s) = \frac{2}{\pi}\left[f(0) + s\int_0^s \frac{f'(\sigma)d\sigma}{\sqrt{s^2-\sigma^2}}\right]. \tag{21}$$

As a result from (21), we have

$$p_{ri}(\rho_i) = \frac{4\omega R_{\max}}{\pi\theta a_c^2}\sqrt{a_{ri}^2-\rho_i^2} + \frac{q_c}{\pi}\arcsin\sqrt{\frac{a_{ri}^2-\rho_i^2}{a_c^2-\rho_i^2}}, \tag{22}$$

$$P_i = \frac{8\omega R_{\max}a_{ri}^3}{3\theta a_c^2} + 2q_c a_c^2\left[\arcsin\frac{a_{ri}}{a_c} - \sqrt{\frac{a_{ri}^2}{a_c^2}\left(1-\frac{a_{ri}^2}{a_c^2}\right)}\right]. \tag{23}$$

Taking into account that $\eta_i = a_{ri}^2/a_{ci}^2$, $q_{ci} = P_i/(\pi a_{ci}^2)$, from Eqs. (22) and (23), we have

$$p_{ri}(\rho_i) = \frac{4\eta_i^{0.5}\omega R_{\max}}{\pi\theta a_c^2}\sqrt{1-\frac{\rho_i^2}{a_{ri}^2}} + \frac{q_c}{\pi}\arcsin\sqrt{\frac{a_{ri}^2-\rho_i^2}{a_c^2-\rho_i^2}}, \tag{24}$$

$$q_{ci} = \frac{8\omega R_{\max}\eta_i^{1.5}}{3\pi\theta a_c} + \frac{2}{\pi}q_c\left[\arcsin\eta_i^{0.5} - \sqrt{\eta_i(1-\eta_i)}\right]. \tag{25}$$

The mean p_{mi} and the maximum $p_{ri}(0)$ stresses at the contact spot are described by equations

$$p_{mi} = \frac{N_i}{A_{ri}} = \frac{q_{ci}}{\eta_i} = \frac{8\eta_i^{0,5}\omega R_{\max}}{3\pi\theta a_c} + \frac{2q_c}{\pi\eta_i}\left[\arcsin\eta_i^{0.5} - \sqrt{\eta_i(1-\eta_i)}\right], \tag{26}$$

$$p_{ri}(0) = \frac{4\eta_i^{0,5}\omega R_{\max}}{\pi\theta a_c} + \frac{q_c}{\pi}\arcsin\eta_i^{0..5}. \tag{27}$$

With sufficient accuracy (with an error of less than 1%), Eq. (24) can be written as.

$$p_r(\eta_i,\rho_i) = p_{r0}(\eta_i,0)\left(1-\rho_i^2/a_r^2\right)^{\beta},\ \beta = p_{r0}(\eta_i,0)/p_m(\eta_i,0) - 1. \tag{28}$$

3.2. The contact of a spherical asperity and the hardenable elastic-plastic half-space

Problems of a spherical asperity elastic-plastic indentation are not studied sufficiently and some suggested solutions are needed for clarification and improvement. One of the important problems is material hardening. The authors' approach to solve this problem is given in Ref. [14].

In several works [15, 16], the empirical Meyer law linking the spherical indentation load and an indenter diameter was used to allow for material hardening in solving the tribomechanic problems. Let us consider this approach at length.

In describing elastic-plastic characteristics of the hardenable material, the Hollomon's power law is widely used. According to it, the relation between the true stress S and the true strain ε under uniaxial tension or compression is described by equations

$$S = \begin{cases} \varepsilon E, & \varepsilon \le \varepsilon_y; \\ K\varepsilon^n, & \varepsilon \ge \varepsilon_y; \end{cases} \tag{29}$$

where E is the elastic modulus and n is the strain-hardening exponent.

The constant K is determined from the equality condition for σ at ε_y. Then the second equation in Eq. (29) can be written as.

$$\frac{S}{\sigma_y} = \left(\frac{E\varepsilon}{\sigma_y}\right)^n = \left(\frac{\varepsilon}{\varepsilon_y}\right)^n, \varepsilon \ge \varepsilon_y. \tag{30}$$

where $\sigma_y \approx S_y$, σ_y is the yield strength, and $\varepsilon_y = \sigma_y/E$.

Taking into accord that the limiting uniform strain $\varepsilon_u = n$, the exponential deformation hardening can be determined according to Ref. [17] from the following equation:

$$n\ln n - n\left(1 + \ln \varepsilon_y\right) - \ln\frac{\sigma u}{\sigma_y} = 0, \tag{31}$$

where σ_u is the tensile strength.

Meyer was the first who described a material behavior in the elastic-plastic domain. He related the load P to the indentation diameter d as

$$P = Ad^m. \tag{32}$$

The empirical Meyer law is often written as:

$$\frac{4P}{\pi d^2} = HM = A^*\left(\frac{d}{D}\right)^{m-2}. \tag{33}$$

where m, A, and A^* are constants. A^* has a dimension of strength.

The equation on the left side is a mean contact area pressure referred to as the Meyer hardness

$$\frac{4P}{\pi d^2} = \frac{P}{\pi a^2} = p_m = HM, \tag{34}$$

where a is the radius of the contact area.

Using [16], we have

$$\frac{P}{E^* R^2} = \frac{2}{k_\sigma \cdot k_n} \left(\frac{n}{e}\right)^n \varepsilon_y^{1-n} \left(\frac{a}{R}\right)^{2+1.041n}. \tag{35}$$

where E^* is reduced elastic modulus, $k_\sigma = 0.333$ for carbon and pearlitic steel, for other materials, the values of k_σ are given in Ref. [18].

$$k_n = \frac{(2+1.041n)^{1+0.5205n}}{(1+1.041n)^{1+1.041n}} (1.041n)^{0.5205n}. \tag{36}$$

The limits of using of Eq. (35) are given in Ref. [16].

As it was indicated in Ref. [16], the obtained results are in good agreement with the experimental data given in Ref. [19], and with the data of FE analysis [20].

Thus, the proposed approach suggests an alternative to a more complex method for describing elastic-plastic penetration of a sphere on the basis of the kinetic indentation diagram [14], which was used in solving problems of elastic-plastic contacting of rough surfaces.

4. Contacting rough surfaces

4.1. Elastic contact of rough surfaces

4.1.1. Relative contact area

Consider the contact of a rough surface with an elastic-plastic half-space using a roughness model for which the function and the density of the distribution of the asperities are described by Eqs. (15) and (16). The displacement of a rough surface in the general case is determined from Eq. (21) under the condition $F(a_{ri}) = 0$:

$$U_0 = uR_{\max} + 2\Theta q_c (a_l - a_c) + 2\omega R_{\max} \frac{a_{ri}^2}{a_c^2} + +2\theta q_c a_c \left(1 - \sqrt{1 - \frac{a_{ri}^2}{a_c^2}}\right). \tag{37}$$

For an asperity contacting at a point, that is, for $a_{ri} = 0$, we have

$$U_0 = \varepsilon R_{\max} + 2\theta q_c (a_l - a_c). \tag{38}$$

Since the value of U_0 is constant for all points of the contact regions, it follows from Eqs. (56) and (38) that

$$\eta_i + \frac{\theta q_c a_c}{\omega R_{\max}} \left(1 - \sqrt{1 - \eta_i}\right) - \frac{\varepsilon - u}{2\omega} = 0. \tag{39}$$

This equation has a solution

$$\eta_i = \frac{\varepsilon - u}{2\omega} - f_q\left(1 + \frac{f_q}{2} - \sqrt{\left(1 + \frac{f_q}{2}\right)^2 - \frac{\varepsilon - u}{2\omega}}\right), \tag{40}$$

where $f_q = \frac{\theta q_c a_c}{\omega R_{\max}}$.

Contour pressure in the joint of a rough surface with a half-space and the relative area are described by equations.

$$q_c = \frac{N}{A_c} = \frac{1}{A_c}\sum_{i=1}^{n_r} q_{ci}A_{ci};\ \eta = \frac{A_r}{A_c} = \frac{1}{A_c}\sum_{i=1}^{n_r} A_{ci}\eta_i. \tag{41}$$

Considering that for this roughness model $A_{ci} = \text{const}$, $A_c = A_{ci}n_c$, and $dn_r = n_c\varphi_n'(u)\,du$, we represent Eq. (41) in the form.

$$q_c(\varepsilon) = \int_0^{\min(\varepsilon,\varepsilon_s)} q_{ci}\varphi_n'(u)du,\ \eta(\varepsilon) = \int_0^{\min(\varepsilon,\varepsilon_s)} \eta_i\varphi_n'(u)du. \tag{42}$$

Taking into account Eq. (25), we have.

$$f_q(\varepsilon) = \frac{\theta q_c(\varepsilon)a_c}{\omega R_{\max}} = \frac{\frac{8}{3\pi}\int_0^{\min(\varepsilon,\varepsilon_s)} \eta_i^{1,5}\varphi_n'(u)du}{1 - \int_0^{\min(\varepsilon,\varepsilon_s)} \Psi_\eta(\eta_i)\varphi_n'(u)du},\ \Psi_\eta(\eta_i) = \frac{2}{\pi}\left[\arcsin\eta_i^{0.5} - \sqrt{\eta_i(1-\eta_i)}\right]. \tag{43}$$

Figure 4 shows the dependences of the relative contact area on the force elastic-geometric parameter f_q.

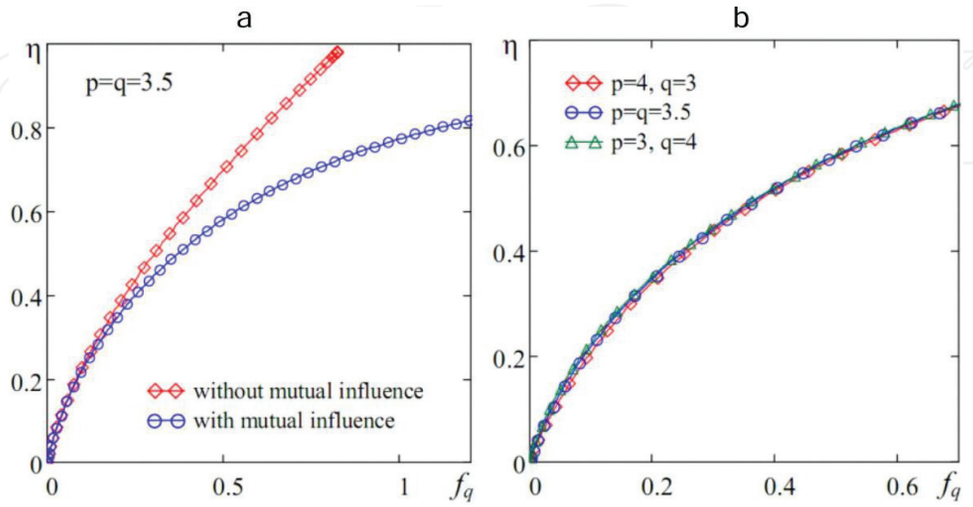

Figure 4. The relative contact area with/without taking into account the mutual influence of asperities (a) and for different values of p and q (b).

4.1.2. Gaps density of the joint

To determine the volume of the intercontact space, it is necessary to determine the volumes of gaps attributable to single contacting and noncontacting asperities [10],

$$V_i = \begin{cases} V_{ri} = 2\pi \int\limits_{a_{ri}}^{a_c} [z_{20}(\rho) - z_{10}(\rho)]\rho d\rho; \\ V_{0i} = 2\pi \int\limits_{0}^{a_{ci}} [z_{2r}(\rho) - z_{1r}(\rho)]\rho d\rho, \end{cases} \tag{44}$$

where z_{10}, z_{20} and z_{1r}, z_{2r} are the equations describing the surfaces of noncontacting and contacting asperities and half-spaces, respectively.

Then, the total volume of the intercontact space at the joint is described by the equation

$$V_c = \sum_{i=1}^{n_r} V_{ri} + \sum_{i=1}^{n_c - n_r} V_{0i}, \tag{45}$$

And the corresponding gap density is equal to

$$\Lambda(\varepsilon) = \frac{V_c}{A_c R_{\max}} = \frac{1}{A_{ci} R_{\max}} \left[\int\limits_{0}^{\min(\varepsilon, \varepsilon_S)} V_{ri} \varphi_n'(u) du + \int\limits_{\min(\varepsilon, \varepsilon_S)}^{\varepsilon_S} V_{0i} \varphi_n'(u) du \right]. \tag{46}$$

Taking into account that $\Lambda_{ri} = V_{ri}/(A_{ci} R_{\max})$ и $\Lambda_{0i} = V_{0i}/(A_{ci} R_{\max})$, it can be represented in the form

$$\Lambda(\varepsilon) = \int\limits_{0}^{\min(\varepsilon, \varepsilon_S)} \Lambda_{ri} \varphi_n'(u) du + \int\limits_{\min(\varepsilon, \varepsilon_S)}^{\varepsilon_S} \Lambda_{0i} \varphi_n'(u) du. \tag{47}$$

We provide the equations of surfaces of the asperities and the half-space that enter into Eq. (44):

$$z_{10} = \omega R_{\max} \left[\frac{\varepsilon - u}{\omega} - x^2 + 2 f_q (k - 1) \right], \tag{48}$$

where $x = \frac{\rho}{a_c}; k = \frac{a_l}{a_c}$,

$$z_{20} = 2\omega R_{\max} f_q \left[k \cdot {}_2F_1\left(-\frac{1}{2}, \frac{1}{2}; 1; \frac{x^2}{k^2} \right) - {}_2F_1\left(-\frac{1}{2}, \frac{1}{2}; 1; x^2 \right) \right], \tag{49}$$

where ${}_2F_1$ is the Gaussian hypergeometric function,

for contacting asperity $z_{1r} = z_{10}$;

$$z_{2r} = \begin{cases} z_{1r}, & 0 \le x < \eta_i^{0,5} \\ U_{Eri} + U_{Eci}, & \eta_i^{0,5} \le x \le 1; \end{cases} \tag{50}$$

$$U_{Eci} = z_{20},\ U_{Eri} = \omega R_{\max} \frac{f_{qi}}{x} {}_2F_1\left(\frac{1}{2}, \frac{1}{2}; \beta + 2; \frac{\eta_i}{x^2}\right),\ f_{qi} = \frac{8\eta_i^{1,5}}{3\pi} + \Psi(\eta_i) \cdot f_q, \tag{51}$$

where $\beta = p_{ri}(0)/p_m - 1$.

Figure 5 shows the different positions of the single asperity in the process of contacting with the rough surface: case *a* corresponds to original position; case *b* corresponds to the touching at a point; and cases *c* and *d* correspond to the contact under the different loads.

Taking into account that $x^2 = t$, we have

$$V_{0i} = \pi a_c^2 \int_0^1 \Delta z_0(t)dt,\ V_{ri} = \pi a_c^2 \int_{\eta_i}^1 \Delta z_r(t)dt. \tag{52}$$

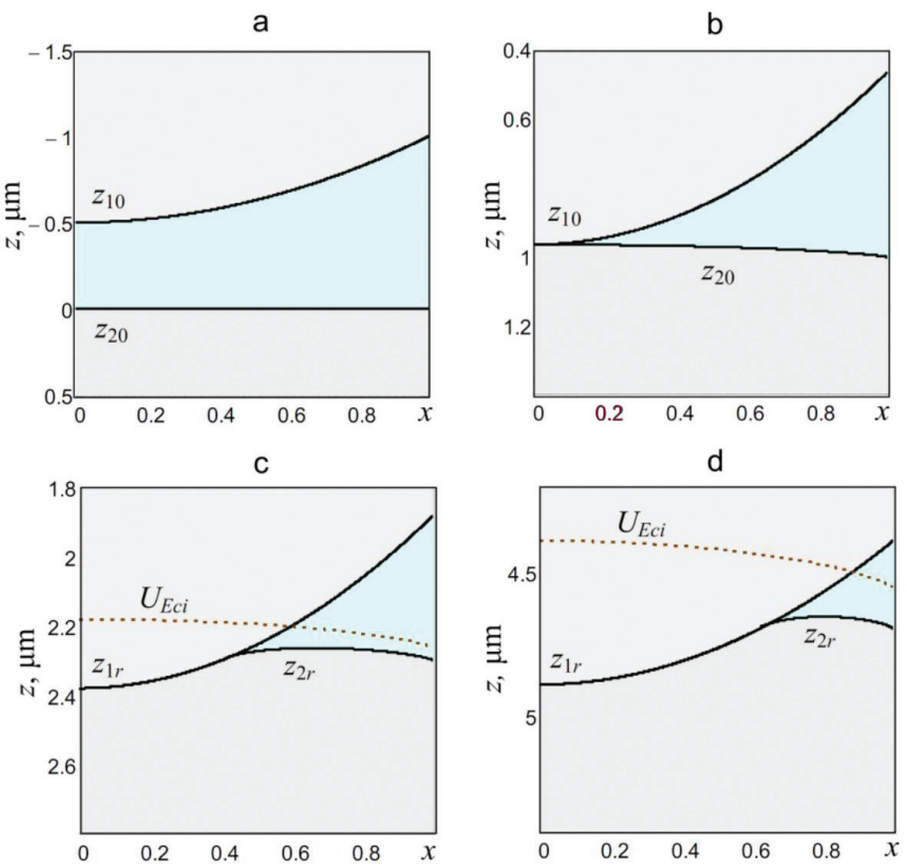

Figure 5. The scheme for contacting a single asperity located at level $u = 0.5$.

where $\Delta z_0 = z_{20} - z_{10}$ and $\Delta z_r = z_{2r} - z_{1r}$.

Since $\Lambda_i = \frac{V_i}{\pi a_c R_{\max}}$, after integrating (52), we have

$$\Lambda_{oi} = \omega\left\{\frac{1}{2} - \frac{\varepsilon - u}{\omega} - 2f_q\left[(k-1) - k\cdot{}_2F_1\left(-\frac{1}{2},\frac{1}{2};2;\frac{1}{k^2}\right) + {}_2F_1\left(-\frac{1}{2},\frac{1}{2};2;1\right)\right]\right\}. \tag{53}$$

$$\begin{aligned}\Lambda_{ri} =& \omega\left\{(1-\eta_i)\left[\frac{1+\eta_i}{2} - \frac{\varepsilon - u}{\omega} - 2f_q(k-1)\right] + 2f_q k\left[{}_2F_1\left(-\frac{1}{2},\frac{1}{2};2;\frac{1}{k^2}\right) - \right.\right.\\ &- \eta_i\,{}_2F_1\left(-\frac{1}{2},\frac{1}{2};2;\frac{\eta_i}{k^2}\right)\Big] - 2f_q\left[{}_2F_1\left(-\frac{1}{2},\frac{1}{2};2;1\right) - \eta_i\,{}_2F_1\left(-\frac{1}{2},\frac{1}{2};2;\eta_i\right)\right] +\\ &\left.\left. + 2f_{qi}\left[{}_2F_1\left(-\frac{1}{2},\frac{1}{2};\beta+2;\eta_i\right) - \eta_i^{0,5}\,{}_2F_1\left(-\frac{1}{2},\frac{1}{2};\beta+2;1\right)\right]\right\}.\end{aligned} \tag{54}$$

Substituting the equations obtained in Eq. (47), we determine the joint density $\Lambda(\varepsilon)$. To determine the dependence $\Lambda\left(f_q\right)$, it is necessary to exclude the parameter ε from the dependences $f_q(\varepsilon)$ and $\Lambda(\varepsilon)$.

Figure 6 shows the dependence of the gap density on the complex parameter f_q when two rough surfaces come into contact. **Figure 2** shows that the contact density does not depend on the parameters p and q, since the dependences for the different values of p and q.

4.1.3. The criteria for the appearance of plastic deformations

To determine the limits of using the above equations for metal surfaces, it is necessary to have a reliable criterion of plasticity. The closest coincidence with the experimental data on the indentation into elastic-plastic media was shown by the energy Mises' theory of shear strain and the theory of the maximum tangential stresses of Tresca. The difference between the two

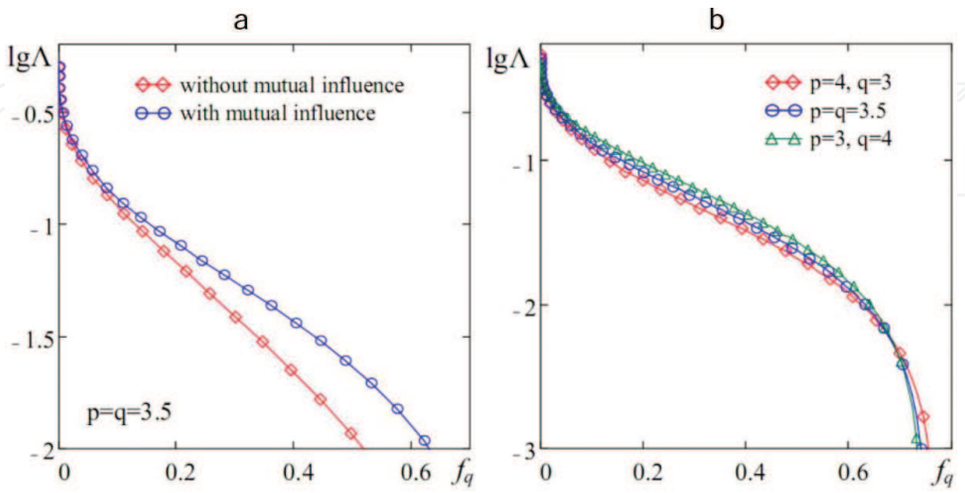

Figure 6. The gap density with/without taking into account the mutual influence of asperities (a) and for different values of p and q (b).

criteria is small; therefore, it is advisable to use the Tresca criterion because of its algebraic simplicity. The problem of determining the plasticity criterion for the considered loading scheme for a single asperity (**Figure 3**) was considered in [21]. In this case, the data of the effect of an axisymmetric load of the form Eq. (28) on the stress-strain state were taken into account. An important conclusion of [21] is the statement of stability of the values of the relative contact area η_{ip} for distributed at different heights asperities, at which plastic deformation begins. Thus, the value of η_{ip} for any asperity loaded according to **Figure 3** can be determined for the highest asperity at $u = 0$, $q_c = 0$, and $\beta = 0,5$.

By the Tresca criterion of the maximum tangential stresses, the plastic deformation on the z axis corresponds to the equivalent stress [22].

$$\sigma_{eq} = 2\tau_{1\max} = 0,62p_0 = \sigma_y. \tag{55}$$

The maximum contact pressure is defined as $p_0 = K_y\sigma_y$, where $K_y = 1,613$. The mean contact pressure is $p_m = K_y\sigma_y/(1+\beta)$.

Using Hertz's expressions for the radius of the contact area.

$$a_{ri} = \left(\frac{3P_i r}{4E^*}\right)^{\frac{1}{3}}, \tag{56}$$

and taking into account that.

$$P_i = \pi a_{ri}^2 p_m,\ r = \frac{a_c^2}{2\omega R_{\max}},\ \frac{a_{ri}^2}{a_c^2} = \eta_i,\ \frac{\sigma_y}{E^*} = \varepsilon_y, \tag{57}$$

We obtain the value of the criterion for the appearance of plastic strains in the near-surface layer

$$\eta_p^* = \left(\frac{3\pi K_y}{8(\beta+1)} f_y\right)^2, \tag{58}$$

where $f_y = \frac{\sigma_y a_c}{E^*\omega R_{\max}}$.

For the highest asperity $\eta_p^* = 1,605 f_y^2$. Thus, the proposed criterion of plasticity does not depend on loading conditions and this is its advantage.

Similarly, we define the criterion of occurrence of plastic deformation at the contact area. According to [23], the equivalent stresses at the center of the area are

$$\frac{\sigma_{eq}(0)}{p_m} = 0,2(1+\beta). \tag{59}$$

The highest value of the equivalent stress $\sigma_{eq}(1)$ is on the contour of the contact area, where it slightly exceeds $\sigma_{eq}(0)$ in the center of the loading area. It is convenient to represent

$\sigma_{eq}(1) = K_\sigma \cdot \sigma_{eq}(0)$, where for $\beta = 0,5$ according to the energy theory of shear strains $K_\sigma = 1,16$, according to the theory of maximal tangential stresses $K_\sigma = 1,33$.

At the moment of appearance of plastic deformation along the contour of the contact area $\sigma_{eq}(1) = \sigma_y$, and the average contact pressure.

$$p_m = \frac{5\sigma_y}{K_\sigma(1+\beta)}. \tag{60}$$

Then, similarly to the above reasoning, the criterion of the appearance of plastic deformations in the contact area is

$$\eta_p^{**} = \left(\frac{15\pi}{8K_\sigma(\beta+1)} f_y\right)^2. \tag{61}$$

For the highest asperity $\eta_p^{**} = 15,42K_\sigma^{-2} f_y^2$. According to the theory of maximum tangential stresses $\eta_p^{**} = 5,405\eta_p^*$, according to the energy theory of shear deformations $\eta_p^{**} = 7,105\eta_p^*$.

4.2. Elastic-plastic contact of rough surfaces

Contact characteristics for elastic-plastic contact will be considered taking into account the mutual influence of the contacting asperities. By analogy with the elastic contact, we assume that the mutual influence of the asperities is equivalent to the action of the additional load q_c (**Figure 3**). We use a discrete roughness model, described by Eqs. (15) and (16).

4.2.1. Relative contact area

According to Eq. (33), the load applied to a single asperity

$$\frac{P_i}{E^* R^2} = \frac{2}{k_\sigma \cdot k_n} \left(\frac{n}{e}\right)^n \varepsilon_y^{1-n} \left(\frac{a_{ri}}{R}\right)^{2+1.041n}. \tag{62}$$

Considering that for the roughness model used $R = a_c^2/(2\omega R_{\max})$ and $\eta_i = a_{ri}^2/a_c^2$, from Eq. (62) we have

$$\frac{q_{ci}}{E^*} = \frac{P_i}{E^* \cdot \pi a_c^2} = \frac{2}{k_\sigma \cdot k_n} \cdot \left(\frac{2\omega R_{\max}}{a_c}\right)^{1.041n} \left(\frac{n}{e}\right)^n \varepsilon_y^{1-n} \eta_i^{1+0.52n}. \tag{63}$$

For elastic-plastic contact, it is convenient to use the parameter $\overline{q}_\sigma = q_c/\sigma_y$, then from Eq. (63) we have

$$\overline{q}_{\sigma i} = \frac{q_{ci}}{\sigma_y} = C_a \cdot \eta_i^{1+0.52n}, \tag{64}$$

where

$$C_a = C_a(\varepsilon_y, n) = \frac{2}{k_\sigma \cdot k_n} \cdot \left(\frac{2\omega R_{\max}}{a_c}\right)^{1.041n} \left(\frac{n}{e \cdot \varepsilon_y}\right)^n. \tag{65}$$

By analogy with Eq. (25), taking into account Eq. (64), for an elastic-plastic contact, we have

$$\overline{q}_{\sigma i} = C_a \cdot \eta_i^{1+0.52n} + \overline{q}_\sigma \cdot \Psi_\eta(\eta_i). \tag{66}$$

In order to preserve the acceptability of the equations for elastic and elastic-plastic contacts, we use the relations.

$$f_q = \frac{q_c a_c}{E^* \omega R_{\max}} = \frac{q_c}{\sigma_y} \cdot \frac{\sigma_y}{E^*} \cdot \frac{a_c}{\omega R_{max}} = \overline{q}_\sigma \cdot f_y; f_y = \frac{\varepsilon_y a_c}{\omega R_{\max}}; f_{qi} = \overline{q}_{\sigma i} \cdot f_y. \tag{67}$$

Then Eq. (66) can be represented in the form

$$f_{qi} = C_a \cdot \eta_i^{1+0.52n} + f_q \cdot \Psi_\eta(\eta_i), \tag{68}$$

where $C_f = C_a \cdot f_y$, η_i is determined by Eq. (40).

Summing up f_{qi} over all asperities, we have

$$f_q(\varepsilon) = \frac{C_f \int_0^{\min(\varepsilon,\varepsilon_s)} \eta_i^{1+0.52n} \varphi_n'(u) du}{1 - \int_0^{\min(\varepsilon,\varepsilon_s)} \Psi_\eta(\eta_i) \varphi_n'(u) du}. \tag{69}$$

For a given value ε, we solve the system of transcendental Eqs. (40), (69) and obtain the dependence $f_q(\varepsilon)$.

Similarly, using Eq. (40) and $f_q(\varepsilon)$, we have

$$\eta(\varepsilon) = \int_0^{\min(\varepsilon,\varepsilon_s)} \eta_i\left(\varepsilon, f_q\right) \varphi_n'(u) du. \tag{70}$$

Excluding the parameter ε from Eqs. (69) and (70), we obtain the dependence $\eta\left(f_q\right)$ or $\eta(\overline{q}_\sigma)$.

Figures 7 and **8** present the dependencies of the relative contact area on the relative force parameter $\overline{q}_\sigma$.

4.2.2. Gaps density of the joint

The scheme of the action of the loads p_r and q_c is similar to the scheme for elastic contact (**Figure 3**).

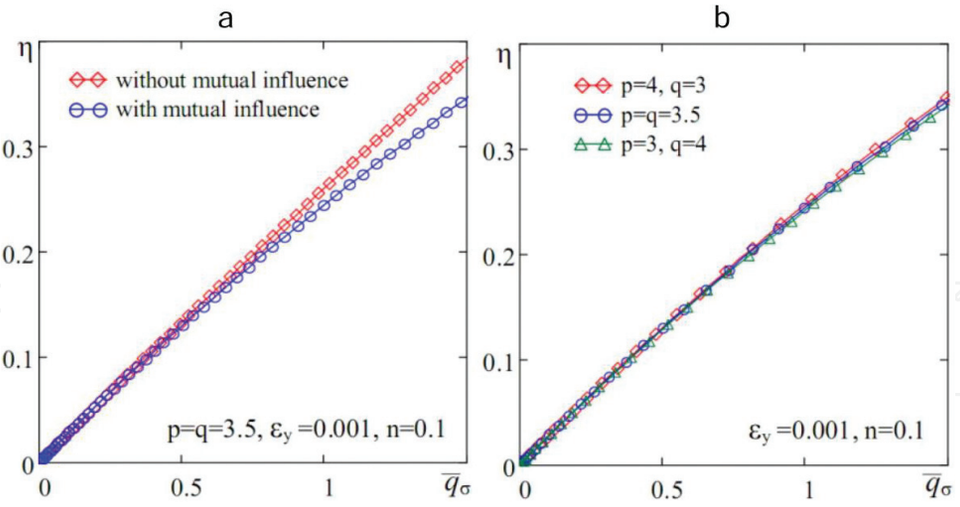

Figure 7. The relative contact area with/without taking into account the mutual influence of asperities (a) and for different values of p and q (b).

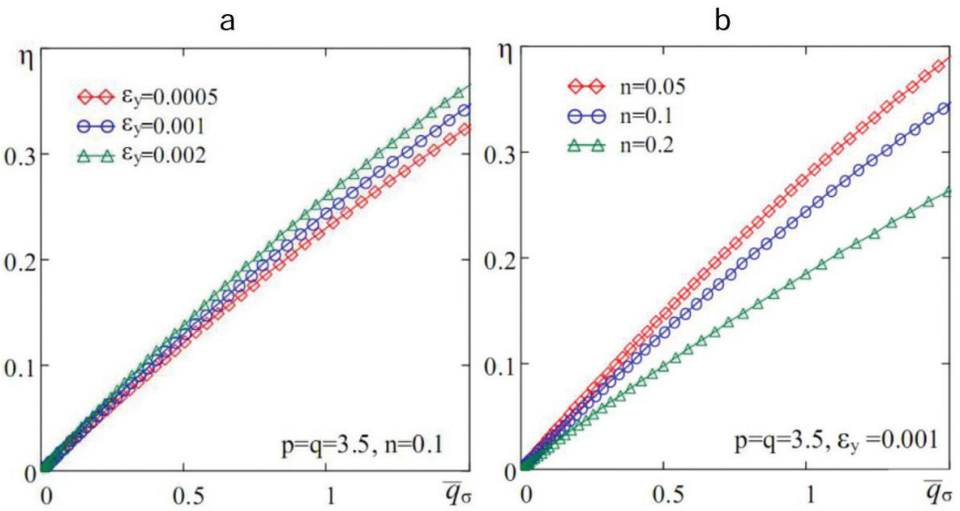

Figure 8. The relative contact area for different values of ε_y and n.

For an elastic-plastic contact

$$\overline{P}_i = \frac{P_i}{E^* R^2} \propto \left(\frac{h_i}{R}\right)^{0,5205n+1}, \tag{71}$$

therefore, the pressure distribution in the contact area described by [4]

$$p(r) = p_0\left(1 - \frac{r^2}{a^2}\right)^{\beta}, \tag{72}$$

where $p_0 = p_m(1+\beta)$ is pressure at $r = 0$, p_m is the mean pressure on contact area and $\beta = 0,5205n$.

Total density of gaps with elastic-plastic contact

$$\Lambda = \Lambda_e - \Lambda_p = \Lambda_{e0} + \Lambda_{er} - \Lambda_p, \tag{73}$$

where Λ_e is the density of gaps due to the elastic punching of the half-space, which accounted for single contacting and noncontacting asperities; Λ_p is reduction of the gap density due to the plastic displacement of the material into the interfacial space.

The value of Λ_e is determined, similarly to the elastic contact, by Eq. (47). In this case, f_{qi} is determined by Eq. (68) and the parameter β is used in Eq. (72).

Let us determine the volume of the displaced material for a single contacting asperity (**Figure 9**).

Let us assume that the unloaded crater has a constant radius R_{fi} and the unloaded depth from the level of the initial surface h_{fi}. The volume of plastically displaced material falling on a single crater is equal to the volume of a spherical segment of height h_f and radius R_{fi}:

$$V_{pi} = \pi h_{fi}^2 \left(R_{fi} - \frac{h_{fi}}{3} \right). \tag{74}$$

The total volume of the displaced material

$$V_p = n_c \int_0^{\min(\varepsilon,\varepsilon_s)} V_{pi} \varphi_n'(u) du. \tag{75}$$

Since $\Lambda_p = V_p/(A_c R_{\max})$, we have

$$\Lambda_p = \omega \int_0^{\min(\varepsilon,\varepsilon_s)} \left(\frac{\eta_i}{c^2} - \eta_i^{-0,5} f_{qi} K_{\beta 0} \right)^2 \left\{ 0,5 \left[1 - \eta_i^{-1,5} f_{qi} \left(K_{\beta 0} - K_{\beta c} \right) \right]^{-1} - \frac{(\omega R_{\max})^2}{3 a_c^2} \times \right.$$
$$\left. \times \left(\frac{\eta_i}{c^2} - \eta_i^{-0,5} f_{qi} K_{\beta 0} \right) \right\} \varphi_n'(u) du. \tag{76}$$

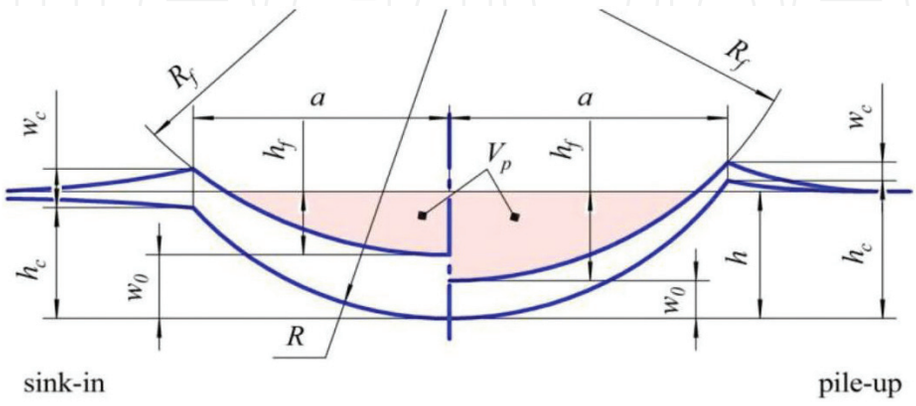

Figure 9. Scheme of the unloaded crater.

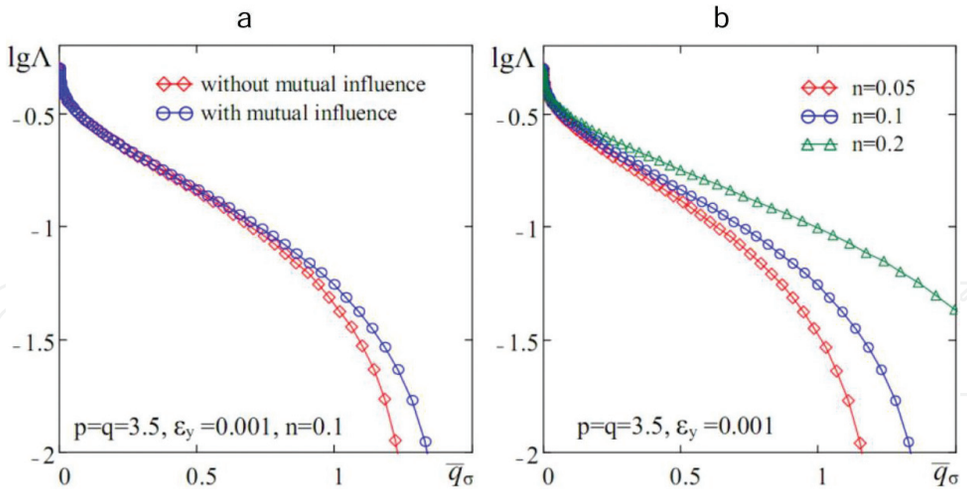

Figure 10. The gap density with/without taking into account the mutual influence of asperities (a) and for different values of p and q (b).

Substituting Eq. (76) into Eq. (73), we find the total gap density for elastic-plastic contact.

Figure 10 presents the dependencies of the gap density on the relative force parameter $\overline{q}_\sigma$.

5. Ensuring specified tightness

Ensuring specified tightness or leakage rate is related to the determination of the force parameters f_q or $\overline{q}_\sigma$. The sealing capacity of the SJ is evaluated by the permeability functional by Eq. (1). The contact characteristics—the relative contact area η and the gap density Λ, included in Eq. (1), are defined in the previous section. Included in Eq. (1), the probability v_k of the medium flowing through the SJ is determined by the fusion of contact spots and is given in Ref. [3]. Two adjacent asperities will merge if $\eta_i > 0.5$for each asperity.

Figure 11 shows the dependences for the elastic and elastic-plastic contacts.

The required permeability functional is determined by [3]

$$C_u^* = \frac{2l\mu G_l^*}{R_{\max}^3 \rho \Delta p}, \tag{77}$$

where G_l^* is the specified tightness; ρ is the density of the sealed medium; p_1 and p_2 are the inlet and outlet pressures; μ is the dynamic viscosity; $\Delta p = p_1 - p_2$; and l is the compacting band width.

The force parameters f_q or $\overline{q}_\sigma$, that providing a given level C_u^* are determined from the $C_u\left(f_q\right)$ or $C_u\left(\overline{q}_\sigma\right)$ (**Figure 11**).

http://dx.doi.org/10.5772/intechopen.72196

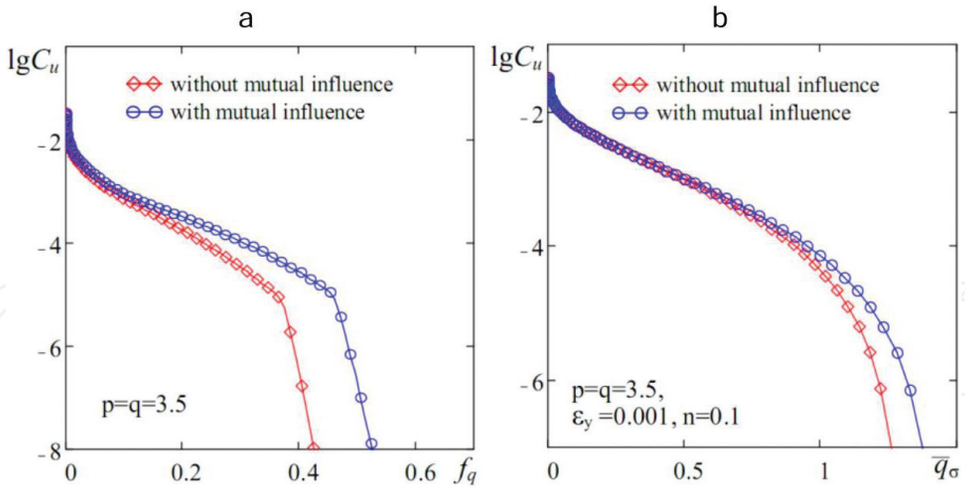

Figure 11. The dependences of the permeability functional for the elastic (a) and elastic-plastic (b) contacts.

6. Conclusion

Using the proposed model of roughness as a result of the studies, methods for determining the contact characteristics and the conditions for ensuring a specified tightness of the joints were developed and established:

1. Contact characteristics and the permeability functional are determined depending on the introduced dimensionless power parameters f_q for the elastic and $\overline{q}_\sigma$ for elastic-plastic contacts.
2. The relative contact area and the gap density for elastic contact do not depend on the values of the parameters of the bearing curve p and q. To a large extent, the mutual influence of asperities affects, and at $f_q > 0.47$, the determining factor affecting the permeability functional is the probability v_k of the medium flowing (**Figure 11**).
3. To describe the elastic-plastic contact, Mayer's law and the relation between the hardening exponent n and the Mayer index m were used.
4. In the case of elastic-plastic contact, the exponent of hardening n has a greater effect on the contact characteristics and to a lesser extent, the parameter ε_y and the mutual influence of the asperities. For the considered range of the parameter $\overline{q}_\sigma$, the fusion of the contact spots is insignificant.

Author details

Peter Ogar*, Sergey Belokobylsky and Denis Gorokhov

*Address all correspondence to: ogar@brstu.ru

Bratsk State University, Bratsk, Russia

References

[1] Greenwood JA, Williamson JBR. Contact of nominally flat sufaces. Proceedings of the Royal Society. 1966;**A295**:301-313

[2] Demkin NB. Contact of Rough Surfaces. Moscow: Nauka; 1970. p. 227

[3] Ogar PM, Sheremeta RN, Lkhanag D. The Tightness of the Metal-Polymeric Joints of Rough Surfaces. Bratsk: BrSU; 2006. p. 159

[4] Ogar PM, Gorokhov DB, Turchenko AV. Contact Mechanics of Rough Surfaces. Brstu: Bratsk; 2016. p. 282

[5] Golubev AI, Kondakov LA, editors. Handbook of Seals and Sealing Equipment. 2nd ed. Moscow: Mechanical Engineering; 1994. p. 448

[6] Goldade VA, Neverov AS, Pinchuk LS. Low-Modulus Composites Based on Thermoplastics. Minsk: Science and Technology; 1984. p. 231

[7] Bartenev GM, Lavrentiev VV. Friction and Wear of Polymers. Moscow: Chemistry; 1972. p. 240

[8] Goryacheva IG, Dobychin NM. Contact Problems in Tribology. Mechanical Engineering: Moscow; 1988. p. 256

[9] Goryacheva IG. Mechanics of Frictional Contact. Moscow: Nauka; 2001. p. 478

[10] Dolotov AM, Ogar PM, Chegodaev DE. Fundamentals of the Theory and Design of Seals Pneumohydraulic Valves of Flying Machines. Moscow: MAI; 2000. p. 296

[11] Ogar PM, Gorokhov DB, Elsukov VK. Elastic contact of a rigid rough surface with the low-modulus half-space. Systems. Methods. Technologies. 2017;**34**:7-12. DOI: 10.18324/2077-5415-2017-2-7-12

[12] Timoshenko SP, Goodyer J. Theory of Elasticity. Moscow: Nauka; 1979. p. 560

[13] Shtaerman IY. Contact Problem of the Theory of Elasticity. Moscow-Leningrad: Gostekhizdat; 1949. p. 270

[14] Ogar PM, Tarasov VA. Kinetic indentation application to determine contact characteristics of sphere and elastic-plastic half-space. Advances in Materials Research. 2013;**664**: 625-631

[15] Ogar PM, Gorokhov DB. Meyer law application for solving problems of surface plastic deformation by spherical indentation. Applied Mechanics and Materials. 2015;**788**:199-204

[16] Ogar P, Gorokhov D. Meyer law application to account of material hardening under rigid spherical indentation. In: Proceeding of 22nd international conference (MECHANIKA 2017). Kaunas: KUT; 19 May 2017. p. 287-290

[17] Ogar PM, Gorokhov DB. Parameters for elastic-plastic body to calculate contact characteristics under the sphere indentation, Systems. Methods. Technologies. 2016;**1**(29):28-32. DOI: 10.18324/2077-5415-2016-1-28-32

[18] Gaško M, Rosenberg G. Correlation between hardness and tensile properties in ultra-high strength dual phase steels – Short communication. Materials engineering - Materiálové inžinierstvo. 2011;**18**:155-159

[19] Kucharski S, Mroz Z. Indentation of plastic hardening parameters of metals from spherical indentation tests. Materials Science and Engineering. 2001;**A318**:65-76

[20] Hernot X, Bartier O, Bekouche Y, El Abdi R, Mauvoisin G. Influence of penetration depth and mechanical properties on contact radius determination for spherical indentation. International Journal of Solids and Structures. 2006;**43**:4136-4153

[21] Ogar PM, Tarasov VA, Turchenko AV. The criterion plasticity for individual asperity when contacting rigid rough surfaces with the half-space. Systems. Methods. Technologies. 2013; **2**(18):29-34

[22] Johnson KL. Contact Mechanics. Cambridge University Press; 1981. p. 452

[23] Ogar PM, Tarasov VA. Influence of the shape of an axisymmetric load on a stress-strain elastically plastic half-space. Systems. Methods. Technologies. 2010;**5**:14-20

IntechOpen